Robotics and Autonomous Systems 143 (2021) 103828

Contents lists available at ScienceDirect

Robotics and Autonomous Systems

journal homepage: www.elsevier.com/locate/robot

Design and characterization of a lightweight underactuated RACA hand exoskeleton for neurorehabilitation

Victor Moreno-SanJuan, Ana Cisnal, Juan-Carlos Fraile, Javier Pérez-Turiel *, Eusebio de-la-Fuente

ITAP (Instituto de Tecnologías Avanzadas de la Producción), University of Valladolid, Faculty of Industrial Engineering, Paseo del Cauce, 59, 47011 Valladolid, Spain

ARTICLE INFO

Article history:
Received 21 January 2021
Received in revised form 18 May 2021
Accepted 7 June 2021
Available online 9 June 2021

Keywords:
RACA robots
Hand exoskeleton
Stroke rehabilitation
Underactuated mechanisms
Mechanical design
Kinematic model

ABSTRACT

The spread of the use of robotic devices in neuro-rehabilitation therapies requires the availability of lightweight, easy-to-use, cost-effective and versatile systems. RobHand has been designed with these goals in mind. It is a hand exoskeleton especially suitable for patients suffering from spasticity in the fingers since it is easy to place in the hand and, from an underactuated design, allows both flexion and extension of the fingers. In this work, the structural characteristics, the mechanical design and the development and validation of the kinematic model of the device are presented, all of which has been carried out taking into account the recommendations of the new IEC 80601-2-78 standard, which formalizes the concept of RACA (Rehabilitation, Assessment, Compensation, Alleviation) robot and addresses aspects of efficiency and safety, essential in this type of equipment.

1. Introduction

Cerebrovascular accidents (stroke) are the second global cause of death: almost 6 million people out of the 56.9 million deaths worldwide in 2016, according to the World Health Organization (WHO) [1]. Most stroke patients survive, but there is often damage to the motor neuron after the acute phase of the disease. Stroke is the third leading cause of disability, and mainly affects individuals at the peak of their productive life [2]. About 70 to 80 percent of the stroke survivors require long term medical care [3] and live with a poor quality of life [4,5]. Approximately 60% of stroke survivors experience upper extremity dysfunction limiting participation in functional activities [6]. Chronic deficits are especially prevalent in the hand where permanent sensory and/or motor disability constitutes a major problem [7]. In fact, finger extension is the motor function most likely to be impaired [8]. Improving hand function to promote functional recovery is a major task for stroke rehabilitation. However, due to the precision and complexity of functions, complete recovery of hand function is difficult and slow in the rehabilitation process.

Rehabilitation training can be categorized into the following stages: acute, convalescence and maintenance. It is understood that the earlier phases of rehabilitation contribute to the recovery of lost abilities and skills [9]. A solution to this problem would be a rehabilitation support system that allowed patients to carry out rehabilitation exercises [10]. The use of robotic devices in rehabilitation is a promising method for the restoration and relearning of motor functions, providing high-intensity, repetitive, task-specific and interactive treatment [11].

The development of exoskeletons for hand rehabilitation has experienced significant growth in recent years. Hand exoskeletons of very different types have been developed based on criteria of: size, weight, degrees of freedom (DoF), flexibility, and handling capabilities. Actuator type, mechanical design and number of degrees of freedom, are very important aspects in the design of hand exoskeleton for rehabilitation. These exoskeleton devices represent new design challenges for rehabilitation engineering since their DoFs must be aligned with the DOFs of the hand joints, in order to improve patient's usability and portability. In addition, these devices must be able to control the position or force applied at each joint [12].

Recently (May 2019), the IEC (International Electrotechnical Commission) has published two standards in the field of medical robotics. One of them (IEC 80601-2-78) is directly applicable to robotic devices for neuro rehabilitation and it is foreseeable that, in the short and medium term, this standard will have an increasing influence on the development, experimentation and commercialization of these equipment. It is part of the IEC 60601 series of standards (Safety and Essential Performance of Medical Electrical Equipment) and it is the result of collaboration between ISO Technical Committee TC299 (Robotics) and IEC SubCommittee IEC/SC 62D (Electromedical equipment).

* Corresponding author.
E-mail address: turiel@eii.uva.es (J. Pérez-Turiel).

https://doi.org/10.1016/j.robot.2021.103828

IEC 80601-2-78 "Medical Electrical Equipment — Particular requirements for basic safety and essential performance of medical robots for Rehabilitation, Assessment, Compensation or Alleviation (RACA)" is applied to medical robots that physically interact with the patient in order to perform one of the four functions addressed in the standard [13]. These devices are the so called RACA robots: "medical robots intended by its manufacturer to perform rehabilitation, assessment, compensation or alleviation, comprising an actuated applied part". Exoskeletons for motor neuro rehabilitation of the upper limb are explicitly contemplated in the document and are, therefore, subject to its recommendations.

After a stroke, many survivors exhibit intrinsic resistance to hand extension in the form of spasticity and/or hypertonia, which leads to a reduction of the hand range of motion (RoM) [14]. Muscle weakness is also present, to varying degrees in the majority of stroke patients [15,16]. In this paper we present the mechanical design and the kinematic analysis and its validation of RobHand, a novel underactuated neurorehabilitation robotic hand exoskeleton. This device is intended to provide paretic patients a mean of rehabilitation to assist and restore hand functions, by repetitive hand opening and closing practice rehabilitation, which leads to improving the range of motion and hand strength.

RobHand consists of a back support platform with four linear actuators (for index, middle, ring and little fingers), and a thumb module with one linear actuator. Each finger is moved by a mechanical subassembly composed by an underactuated linkage-rotate mechanism (with one intermediate piece and two rods: proximal and distal), which joints with a flexible double-ring, and transmits the force of the linear actuator to the patient's finger during neurorehabilitation tasks. The link lengths of each mechanical subassembly have been designed to cover the workspace of the finger joints, in order to achieve the highest performance in the force transmission between the linear actuator and the finger and to allow flexion and extension finger movements.

The special characteristics of mobility and variety of thumb size, led us to design a specific thumb mechanical module to properly position both, the linear actuator and the mechanical elements necessary to perform the thumb flexion and extension.

Due to hypertonia (spasticity), the paretic hand of hemiplegic patients is clasped into a fist at resting state. To ensure that the device can be easily placed in paretic hands a flexible double-ring link has been designed that allows the MCP and PIP movements. Flexible double-ring sets with three diameter sizes have been constructed to adapt the device to the different human finger sizes (length and thickness).

Due to the limited range of movements, a problem that arises when using an underactuated mechanism is the difficulty of achieving, with the same mechanical configuration, both clamp (flexion) movements and finger extensions or hyper-extensions. In our case we have used the kinematic model to refine the mechanical design of the parts and to ensure that the current version allows both types of movement.

As mentioned previously, one of the most relevant aspects in the new IEC standard is the introduction and formalization of the concept of Actuated Applied Part (AAP), defined as: "Applied Part that is intended to provide actively controlled physical interactions with the patient, that are related to the patient's movement functions, to perform a clinical function of a RACA robot" [13]. RobHand's kinematic model explicitly contemplates the calculation of the parameters associated with the AAPs of the device, which makes it easier to define the distribution of forces and torques exerted and, thus, optimize the interaction with the patient, improving safety in the use of the equipment. We consider this a novel approach and that our study is one of the first applications of the IEC 80601-2-78 standard to a real system.

The rest of the paper is organized as follows: Section 2 shows related work, emphasizing underactuated designs and the constraints posed by spasticity. Section 3 describes the design requirements of RobHand. Section 4 presents the development of the kinematic model including the aspects related to the IEC standard. Section 5 details the mechanical structure of the device, from which the kinematic model is validated in Section 6. Finally, Section 7 discusses the results and conclusions and future work are presented in Section 8.

2. Related work

In the last five years, numerous bibliographic reviews have been published about the application of robotic devices in the rehabilitation of the upper limb [17,18]. Among them there are studies that contemplate the whole range of designs [19] while others focus on the use of exoskeletons [20]. In the case of this type of devices, three reviews have been published on the specific use of exoskeletons for hand rehabilitation just in the last year [21–23]. These studies analyze different aspects such as mechanical design, type of actuators and transmissions used, control strategy, etc. Some of these devices are commercially available such as CyberGrasp [24], Hand of Hope [25] and Gloreha Sinfonia [26].

Some recent proposals include relevant features. In [27] a new exoskeleton for hand rehabilitation with a user-centered design concept, which integrates the requirements of practical use, mechanical structure, and control system, is presented. In [28], a hand robot prototype was developed, with a modularized structure with nine degrees of freedom for the independent control of the patient's fingers. [29] presents the design of an assistive exoskeleton device for the hand, in which finger movements are powered from the palmar side. In [30,31] a novel 2-DOF linkage mechanism driven by two independent actuators allows providing the desired finger motion. The design facilitates adaptation to users with different hand sizes, through a system of slotted holes that allows the device to be precisely adjusted. Other frequently cited systems that have made relevant contributions in this field are HEXORR (The Hand Exoskeleton Rehabilitation Robot) [32], HANDEXOS [33] and HWARD [34].

When the cost of the device and the ease of use are relevant factors, several aspects must be taken into account. In general, the cost of assistive devices increases considerably with the use of non-electric actuators (e.g. pneumatic), multiple motors and sophisticated sensors. The incorporation of these components also contributes to increasing the total weight of the device, making it less comfortable for the patient [17]. Underactuated hand exoskeletons are characterized for utilizing fewer actuators than the number of DoFs, by introducing extra mobility to the mechanism through passive joints and/or elastic elements [35]. Underactuated designs usually contain 1∼5 actuators (compared to the 34 muscles that control the human hand). They offer several advantages [36] as simpler electromechanical structure, lower weight, size and price and simpler control architecture. The underactuation concept has been widely applied to prosthetic hand devices [37]. Each finger is controlled by a single linear actuator that acts on MCP (metacarpophalangeal) and PIP (proximal interphalangeal) joints, while DIP (distal interphalangeal) joint is neglected. The proposed hand exoskeleton uses linkages to power transmission, obtaining 2 DoFs (one active and one passive) for each finger in order to control the flexion and extension angles (MCP and PIP joints angles) of the finger phalanges, whose motion is therefore kinematically coupled.

Improving the design and control of underactuated exoskeletons for hand rehabilitation is currently an active research topic. In [38] KULEX-hand, an underactuated hand exoskeleton for

grasping power assistance for patients having a partially paralyzed hand or the elderly with weakened muscle strength, is described. In [39] the design and the kinematic optimization of an underactuated linkage-based robotic hand exoskeleton to assist users performing grasping tasks is described. In [40], a hand exoskeleton with a high degree of underactuation is introduced: five DoFs of the thumb are moved by just one linear actuator.

Spasticity is the result of an imbalance in the inhibitory and excitatory activity of motor neurons, which causes excessive muscle contraction. The incidence and prevalence values of spasticity vary according to the pathology causing it. In the case of stroke, there are studies that estimate around 38 or 40% of patients will have some degree of spasticity [41]. These values change depending on the evolution in recovery and vary between 27% after one month and more than 40% in the chronic phase [42]. The additional difficulties for functional rehabilitation posed by the presence of spasticity are reflected in the results of a recent clinical study on the use of soft robotic devices for hand rehabilitation in chronic stroke patients [43]. It concludes that these devices could be effective for the functional recovery of upper limb in chronic stroke subjects with mild or no spasticity.

In the literature, several studies can be found using devices specially designed for the assessment of upper limb spasticity. [44] and [45] present exoskeletons specifically designed to assess hand spasticity. An extensive review has recently been published collecting different technological approaches with this objective [46]. However, there are very few treatment and rehabilitation devices whose design has explicitly taken into account the possibility of patients suffering from spasticity. In [47] a specific device for the treatment of spasticity is presented. It is a stretching device consisting of a resting hand splint, a finger and thumb stretcher, and a frame able to fix the middle forearm, wrist joint and proximal portion of metacarpophalangeal [MCP] joints of the fingers. Gloreha Sinfonia [26] is a soft glove type device actuated through five cables that apply the corresponding forces to the distal phalanx. The soft glove design makes difficult to place the device in the hand of patients with severe spasticity. DexoHand, is a cable-actuated exoskeleton that allows patients with spasticity to move their fingers and includes sensors in the cables so that actuator provided forces can be measured [47]. Usability testing has been conducted with both healthy subjects and patients with varying degrees of spasticity, and the authors plan to conduct functional rehabilitation trials with patients. Both by mechanical design, as well as by the use of the underactuation strategy and the control of opening and closing of the device from EMG signals, Hand of Hope (HoH) is an exoskeleton for hand rehabilitation with a very similar approach to ours. However, it is not suitable for the rehabilitation of patients with spasticity in the hand, who must be able to not only perform fingers flexion but also achieve a certain degree of hyperextension [48]. In the case of HoH, the range of motion of the fingers goes from the position of full extension to a maximum of 55° of flexion at the metacarpophalangeal (MCP) joint [49], which is insufficient for the treatment of spastic patients.

3. Design requirements of RobHand

The human hand is highly articulated, leading to complex kinematics. Four fingers (index, middle, ring and little) contain, from the fingertip to the palm of the hand, three phalanges: the distal, the medial (or intermediate), and the proximal phalanx (See Fig. 1). They are connected by joints: distal interphalangeal (DIP), proximal interphalangeal (PIP) and metacarpophalangeal (MCP). DIP (1DoF) and PIP (1DoF) only have flexion/extension movements. MCP (2DoFs) is a joint with the flexion/extension and abduction/adduction movements. The thumb finger has only two

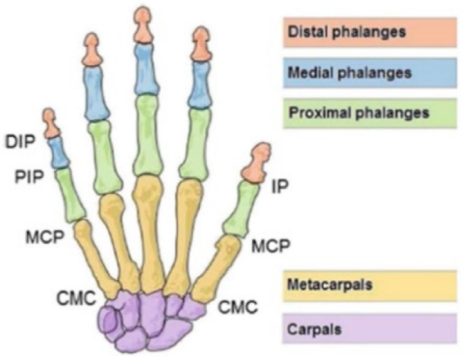

Fig. 1. Human left hand structure [51].

phalanges (proximal and distal) and two joints (MCP and IP). As in the others fingers, the MCP has 2DoFs and the IP has 1DoF. Thumb's motion is also generated by the carpometacarpal (CMC) joint. This joint allows a wide range of movements, including flexion and extension, abduction and adduction, circumduction, and opposition. In total, the human hand has 19 joints and 23 DoFs [50]. For design purposes we have modeled the human hand in a simplified manner considering only a planar scheme. That is, only finger flexion/extension movements have been considered (see Fig. 2), neglecting abduction/adduction movements. The device is only in contact with the proximal and medial phalanges, leaving the distal phalanx free and provides assistance to the MCP (α angle) and PIP (γ angle) joints of the five fingers. In addition, the angle between the middle phalanx and the horizontal is defined as β, necessary for the formalization of the kinematic model. Positive angles are considered for finger extension movement, and negative angles for finger flexion movement.

The design requirements for RobHand were collected from an in-depth review of the literature and discussions with biomedical engineers, physical therapists and rehabilitation doctors. These requirements are:

- **Light-weight (< 750 g) and compact design.** It is fundamental to minimize the weight of the parts of the exoskeleton which are mounted on the hand to avoid creating large forces and torques which negatively affect the patient. Some research claims that the maximum acceptable weight on the hand is in the order of 400 to 500 g [33], and exoskeletons considered well-developed tend to be in a range of 250–500 grams [52] A kinematic design based on the underactuation concept (a single actuator for each finger) minimizes weight and volume of the device.
- **Cost affordable (< 2.000 €).** It must be economically viable for hospitals, rehabilitation clinics and even the patients themselves. There is a need to facilitate at-home rehabilitation because post-stroke programs typically consist of 3-one-hour sessions per week ending after 6 months of the incident [53]. One challenge is the implementation of an affordable rehabilitation platform for domestic environments, which necessarily implies the integration of low-cost technological solutions, while providing safe and intensive training
- **Range of motion (ROM).** The mechanical elements must be designed to allow the natural range of motion of the joints of a healthy human hand (Table 1), and to ensure that the device emulates accurately the kinematics of physiological trajectories. It must act on all fingers of the hand independently, including the thumb and must allow both flexion and hyper-extension movements of the fingers.

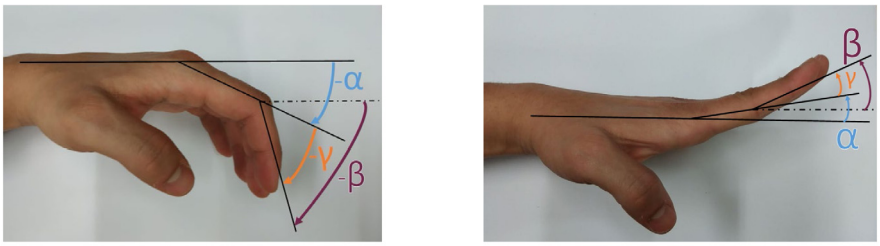

Fig. 2. Hand finger: flexion (A) and extension (B) movements. Sing convention used for MCP and PIP joint angles.

Table 1
RoM for hand finger joints [56].

Finger	Joint angle	Flexion (degrees)	Extension (degrees)
Index	MCP [α]	−90	30 ∼40
	PIP [γ]	−110	0
Middle	MCP [α]	−90	30 ∼40
	PIP [γ]	−110	0
Ring	MCP [α]	−90	30 ∼40
	PIP [γ]	−120	0
Little	MCP [α]	−90	30 ∼40
	PIP [γ]	−135	0
Thumb	MCP [α]	−75 ∼-90	15
	IP	−75 ∼-80	0

- **Easy-of-use**. Easy placement and removal from the patient's paretic hand (we consider that it should be made in less than two minutes). Easy to fit on the back of the hand.
- **Adaptability**. Adjustable without effort to different hand sizes and totally adaptable to the different lengths and thickness of the fingers, including the thumb.
- **Safe**. It must ensure the safety of the patient using mechanical limits of movement related to the natural range of motion (RoM) of the hand finger joints (Table 1). Furthermore, for a hand exoskeleton with rigid linkages, the designer should ensure that the rotation center of the linkage structure coincides with the rotation axis of the human body joint. Otherwise, the different rotational axes may lead to a collision between the user's hand and the device, causing harm to the user's hand [54]. Therefore, the primary concern in the mechanical design of a hand exoskeleton is the coincidence of the centers of rotation [55].
- **Comfort**. The mechanical design must take into account the comfort of the patient by integrating materials and shapes that make the physical interaction and the trajectories made by the patient's fingers comfortable.

4. Kinematic model

The hand is a complex functional limb including over 30 muscles and more than 20 joints that allow performing a wide range of activities with a high level of precision. Kinematics is essential for hand functioning [57]. It is important to bear in mind that, in order to guarantee user safety, human-exoskeleton kinematic compatibility must be guaranteed in the design phase and before undertaking other stages of development [58]. If this compatibility is not achieved, unwanted interaction forces may appear, mainly due to the misalignment between the exoskeleton and the human limbs, whose effect could not be compensated by the device actuators [59]. A kinematic model has been developed by defining mechanical closed loops with a set of equations. They provide the values of the MCP [α] and PIP [β] joints angles of each finger, as function of the stroke extension of the linear actuator.

In order to obtain the kinematic model, each finger is modeled as a planar bar-linkage mechanism, as shown in Fig. 3. In this mechanism all joints between the different parts are taken as rotational joints, with the exception of the motor that constitutes a prismatic or longitudinal joint. Angles and distances of this mechanism are calculated taking as origin of the coordinate system the point of intersection between the back support platform and the intermediate piece, as is shown in Fig. 3.

To determine the number of degrees of freedom, Grubler's Method [60] has been applied. For a planar bar-linkage mechanism of one finger, Grubler's equation states that:

$$DoF = 3\,(N-1) - 2R_1 - R_2 \tag{1}$$

where:

- N: overall number of links in the planar bar-linkage mechanism. In our mechanism N=7+1. There are 7 links and the ground.
- R_1: number of one-DOF kinematic pairs (joints). In our mechanism $R_1 = 10$, as can be seen in Fig. 3.c.
- R_2: number of two-DOF kinematic pairs (joints). In our mechanism $R_2 = 0$.

Applying equation (1) we get DoF = 1, for the planar bar-linkage mechanism of one finger. The lineal parameters that characterize a planar bar-linkage mechanism are shown in Fig. 3.c. The most important are:

- Human finger parameters: L_2, L_3, L_4 and L_8, where L_4 represents MCP — PIP distance. L_8 is the PIP-DIP distance, except for the thumb, where L_8 is the length of the distal phalanx.
- Rod lengths: L_7 (distal) and L_{11} (proximal).
- Intermediate piece parameters: L_{12}, L_{13}, L_{14}, L_{15}.
- d: stroke extension of the linear actuator. It is the distance between P_{12} and R_{23}.
- L_{motor}: closed length of the lineal actuator
- L_{eq}: L_{motor} + d

Geometric parameters that characterize the finger in the planar bar-linkage mechanism of one finger are: L_2, L_3, L_4 and L_8, as can be seen in Fig. 3.c. L_2 and L_3 are the horizontal (X coordinate) and vertical (Y coordinate), distance between the MCP joint and the rotation point of the intermediate piece, respectively.

The prototype incorporates Actuonix L12 linear actuators with 30 mm linear stroke. The mechanical characteristics of RobHand make it impossible for the value of the variable "d" to take values between 0 and 30 mm; but the minimum distance between the points P_{12} and R_{23} will be 16.5 mm and the maximum 39.7 mm. Therefore, parameter "d" is ranging from 16.5 mm to 39.7 mm in our prototype.

The angular parameters that characterize the planar bar-linkage mechanism are shown in Fig. 3.d. MCP [α] and PIP [β]

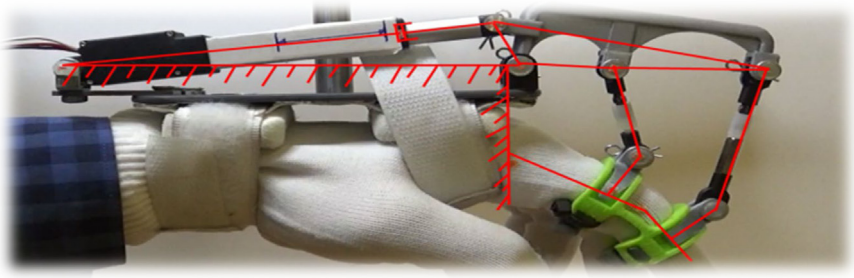

a. RobHand mechanism for one finger

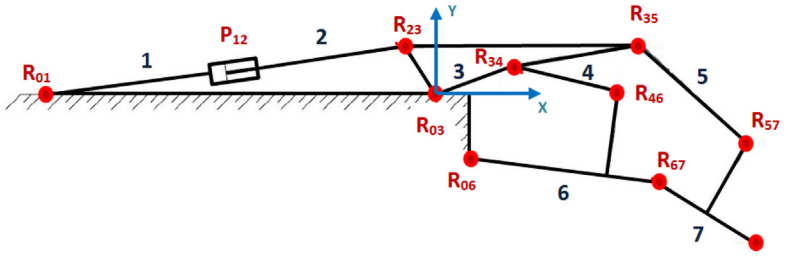

b. Joints with one DoF

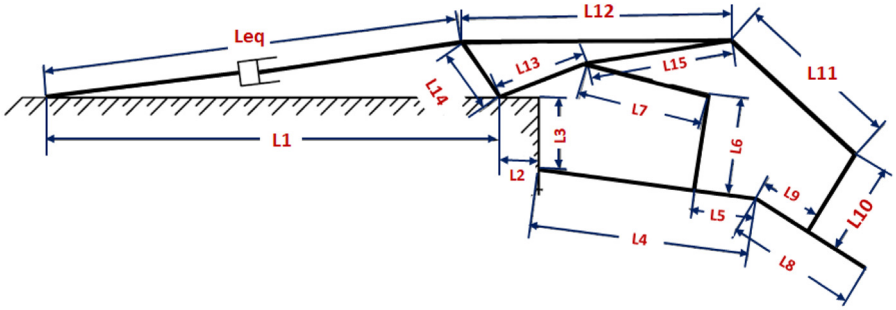

c. Linear parameters

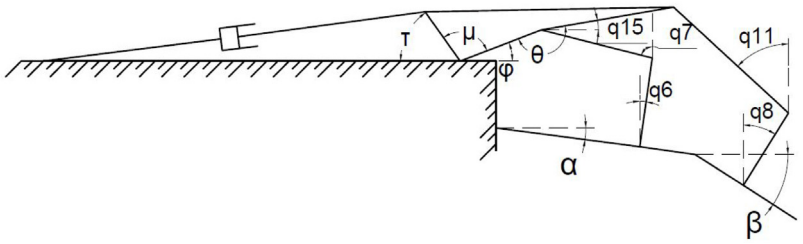

d. Angular parameters

Fig. 3. Representation of the planar bar-linkage mechanism of one finger.

joints angles are the most important angular parameters to study in the kinematic model.

The kinematic analysis has been performed using a set of vector equations by defining two mechanical closed loops. Fig. 3.b and 3.c indicate the linear and angular parameters of RobHand used to define the closed loops showed in Figs. 4 and 5.

Loop 1:

Fig. 4 Shows the first closed loop for determination of MCP joint (α).

The vector loop equations for this loop are:

$$\bar{l}_2 + \bar{l}_3 + \bar{l}_4 - \bar{l}_5 + \bar{l}_6 + \bar{l}_7 + \bar{l}_{13} = 0 \tag{2}$$

$$\begin{cases} X\ axis: & \bar{l}_2 + (\bar{l}_4 - \bar{l}_5)\cos\alpha + \bar{l}_6 \sin q_6 + \bar{l}_7 \sin q_7 \\ & -\bar{l}_{13}\cos\varphi = 0 \quad \text{(a)} \\ Y\ axis: & -\bar{l}_3 + (\bar{l}_4 - \bar{l}_5)\sin\alpha + \bar{l}_6 \cos q_6 + \bar{l}_7 \cos q_7 \\ & -\bar{l}_{13}\sin\varphi = 0 \quad \text{(b)} \end{cases} \tag{3}$$

Fig. 3.d. shows that $\alpha = q_6$. The matrix development of Eqs. (3)(a) and (3)(b) allows us to obtain expression (6), which gives us the angular velocity of the MCP joint ($\dot{\alpha}$). Variables $\{\varphi, \alpha, q_7\}$ are taken, with φ being the independent variable, and $\{\alpha, q_7\}$ dependent variables.

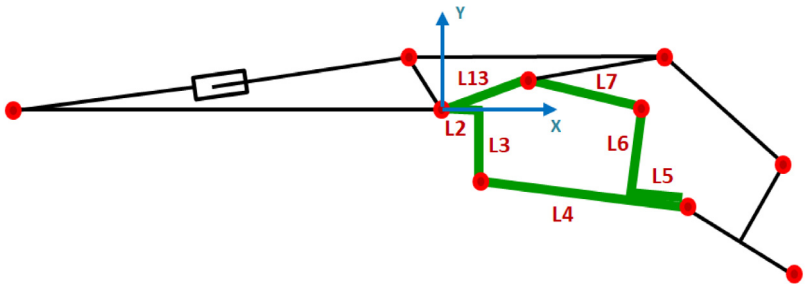

Fig. 4. Kinematic study of the exoskeleton: Loop 1.

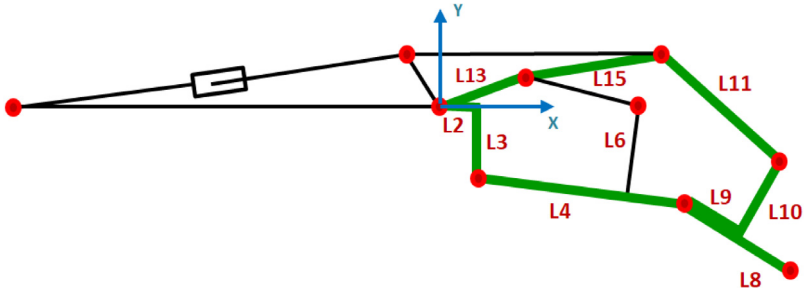

Fig. 5. Kinematic study of the exoskeleton: Loop 2.

Loop 2:

Fig. 5 shows the second vector closed loop for determination of PIP joint (β)

$$\bar{l}_2 + \bar{l}_3 + \bar{l}_4 + \bar{l}_9 + \bar{l}_{10} + \bar{l}_{11} + \bar{l}_{15} + \bar{l}_{13} = 0 \tag{4}$$

$$\begin{cases} X\ axis: & \bar{l}_2 + \bar{l}_4 \cos\alpha + \bar{l}_9 \cos\beta - \bar{l}_{10} \sin q_8 \\ & +\bar{l}_{11} \sin q_{11} - \bar{l}_{15} \cos q_{15} - \bar{l}_{13} \cos\varphi = 0 \quad \text{(a)} \\ Y\ axis: & -\bar{l}_3 + \bar{l}_4 \sin\alpha + \bar{l}_9 \sin\beta + \bar{l}_{10} \cos q_8 \\ & +\bar{l}_{11} \cos q_{11} - \bar{l}_{15} \sin q_{15} - \bar{l}_{13} \sin\varphi = 0 \quad \text{(b)} \end{cases} \tag{5}$$

Fig. 3.d. shows that $\beta = q_8$. The matrix development of Eqs. (5)(a) and (5)(b) allows us to obtain expression (7), which gives us the angular velocity of PIP joint ($\dot{\beta}$). Variables $\{\varphi, \beta, q_{11}\}$ are chosen, with φ being the independent variable, and $\{\beta, q_{11}\}$ dependent variables.

The two systems of kinematic equations (3)(a), (3)(b), (5)(a), (5)(b), taken from the vector closed loops can be derived by using Euler's Identity, obtaining the angular velocity of MCP joint ($\dot{\alpha}$, Eq. (6)) and PIP joint ($\dot{\beta}$, Eq. (7)). The adopted sign convention for MCP and PIP angles is shown in Fig. 2.

$$\dot{\alpha} = \frac{\dot{\varphi}}{(l_4 - l_5)\cos(\alpha - q_7)}(l_{13} \sin q_7 \ \sin\varphi + l_{13} \cos q_7 \cos\varphi) \tag{6}$$

$$\dot{\beta} = \frac{\dot{\varphi}}{l_9 \cos(\beta - q_{11})}(l_{13} \sin q_{11} \sin\varphi + l_{13} \cos q_{11} \cos\varphi) \tag{7}$$

Position of PIP and DIP joints are given by Eqs. (8) and (9):

$$\begin{cases} PIP_X = l_2 + l_4 \cos\alpha \\ PIP_Y = -l_3 + l_4 \sin\alpha \end{cases} \tag{8}$$

$$\begin{cases} DIP_X = l_2 + l_4 \cos\alpha + l_8 \cos\beta \\ DIP_Y = -l_3 + l_4 \sin\alpha + l_8 \sin\beta \end{cases} \tag{9}$$

Taking into account the linear parameters (Fig. 3.c) and angular parameters (Fig. 3.d) of RobHand, MCP [α] and PIP [β] joints angles of each finger are computed, as function of the stroke extension of the linear actuator L_{eq}. First τ must be calculated as indicated in Eq. (10):

$$\tau = \text{acos}\left(\frac{{l_{14}}^2 + {l_1}^2 - {L_{eq}}^2}{2 l_{14} l_1}\right) \tag{10}$$

The value of μ is constant and known, since it is determined by the geometry of the intermediate piece. We determine φ using Eq. (11):

$$\varphi = \pi - \mu - \tau \tag{11}$$

Once φ is known, the value of MCP joint [α] is computed by solving the system of Eqs. (3)(a) and (3)(b), from loop 1. α known, PIP joint [β] is calculated by solving the system of Eqs. (5)(a) and (5)(b) of loop 2. The algorithm to determine the kinematic model is given in Fig. 6. It has been programmed using Matlab®R2019a software.

The first step to determine the kinematic model is to provide the device's kinematic parameters. Then, it is necessary to provide the values of the geometric parameters that characterize the human's finger (L_2, L_3, L_4 and L_8). The size of the hand fingers is variable, depending on people's age, height and physical complexion. The fingers dimensions are based on data obtained from [61], which contains an anthropometric study of the hand for a population sample of 500 people to determine representative part dimensions.

Once all the above-mentioned values have been entered, the kinematic model computes the values of rods length, proximal L_7 and distal L_{11}. Next, considering that the linear actuator performs a path d_i, i = 16.5, ..., 39.7 mm, with $\Delta d = 0.5$ mm, the kinematic model calculates MCP and PIP joint angles (α_i, β_i angles, respectively), as well as the values of the X and Y coordinates of PIP (PIP_X, PIP_Y) and DIP (DIP_X, DIP_Y) points. Finally, all calculated values are stored to be used in the kinematic model validation.

Although the kinematic model has only been presented for the index finger, it is applicable to all fingers since it is parameterizable. The particular anthropomorphic characteristics of the thumb, that only has two phalanges, requires to correctly interpret the results of Eqs. (8) and (9): the coordinates of the PIP and DIP joints of the fingers correspond to the coordinates of the IP joint and fingertip of the thumb, respectively. Fig. 7 shows the

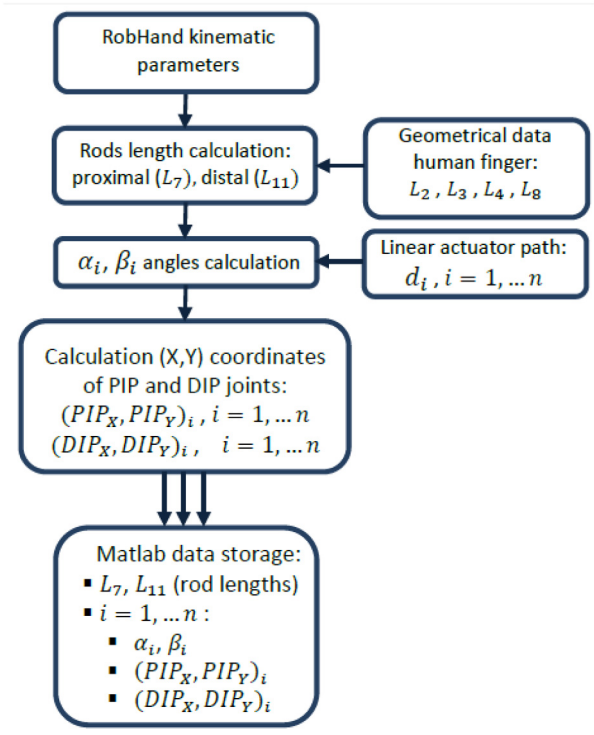

Fig. 6. Algorithm to calculate RobHand kinematic model.

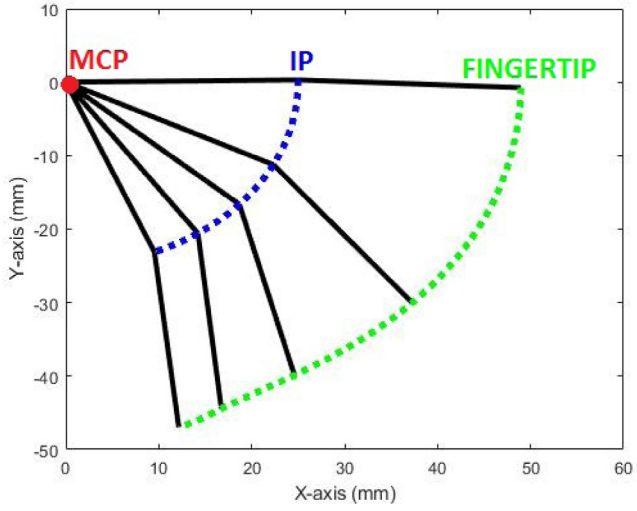

Fig. 7. Range of motion of the IP joint and fingertip of the thumb using the exoskeleton.

path followed by IP joint and fingertip of the thumb in the XY-plane. Since the thumb only has two phalanges, it is possible to determine the trajectory followed by the whole finger. This does not apply to the rest of the fingers whose fingertip trajectories are unknown because the distal phalanges are not actuated.

Study of RobHand's Actuated Applied Parts (APPs) kinematic parameters

The new IEC international standard about RACA robots introduces a classification of the different components of the therapeutic scenario that incorporates a robot. Four different elements must be identified: patient, actuated applied parts (AAPs), actuation system and support system. The standard recommends that the velocity of the AAPs and the forces applied to the patient should be known. Fig. 8 shows the four elements in the rehabilitation scenario regarding RobHand and identify them.

It is important to highlight that the main function of the AAPs is to provide actively controlled physical interaction with the patient, in order to perform the clinical function of the robot. The control of this interaction is usually the result of a shared autonomy between the robot's control system and the actions taken by the patient (or in a generic case, by an external operator, such as a therapist). These interactions can take different forms, from a classic position or force control to impedance, admittance or other control modalities to regulate this interaction. This shared control approach is common in rehabilitation robots and rare in other types of medical robots. According to the standard this is a very important aspect when addressing general security because it allows dealing with "unintended motions" which may result from the interaction between the robot and the patient.

In this sense, it is essential to accurately identify the kinematic parameters associated with the AAPs, to be able to determine the points of exchange of forces and torques between the exoskeleton and the patient. An adequate dynamic analysis that takes into account both performance and efficiency aspects, and security requirements must be carried out.

From the analysis of the mechanical structure of the exoskeleton we conclude that the kinematic parameters of the AAPs are associated with the points of attachment of the finger rings to the mechanism. These points should lead to the knowledge of the movement of the actuated applied parts, and the forces that are transferred to the patient. R_{46} and R_{57} (see Fig. 3.b) were identified as new study points, as it is indicated in Fig. 9.

R_{46} allows us to know how the proximal phalanx's flexible ring behaves. R_{57} shows us how the middle phalanx's flexible ring moves. Taking into account the linear and angular parameters of RobHand, showed in Fig. 3.b and 3.c, we can determine the X and Y coordinates of these points by using Eqs. (12) and (13):

$$\begin{cases} X_{R46} = l_2 + (l_4 - l_5)\cos\alpha + l_6 \sin\alpha \\ Y_{R46} = -l_3 + (l_4 - l_5)\sin\alpha + l_6 \cos\alpha \end{cases} \tag{12}$$

$$\begin{cases} X_{R57} = l_2 + l_4 \cos\alpha + l_9 \cos\beta - l_{10} \cos\beta \\ Y_{R57} = -l_3 + l_4 \sin\alpha + l_9 \sin\beta + l_{10} \cos\gamma \end{cases} \tag{13}$$

With this information, it is possible to extend the previous study to the AAPs and calculate their relevant kinematic parameters. This is essential, in accordance with the approach introduced by the IEC standard, so that the design is consistent with the levels of efficiency and the strict requirements of safety that are necessary in a device that is intended for neuromotor rehabilitation.

5. Structural design

The mechanical structure is composed of five subassemblies, each one associated to one finger. The subassemblies of the index, middle, ring and little fingers are mounted on a platform which is located on the back of the hand. Subassembly for the thumb is mounted on a separate module connected with the back support platform through an off-the-shelf linkage device. Each subassembly includes an underactuated linkage-rotate mechanism composed by three links (see Fig. 10): one intermediate piece and two rods (proximal and distal), and a flexible double-ring. Links transmit the force of the linear actuator up to the flexible double-rings, while the rings connect the exoskeleton to the proximal and medial phalanges (RobHand_VC1.mp4 is a short video clip showing the RobHand platform). The dimensions of the intermediate piece and the two rods have been calculated using

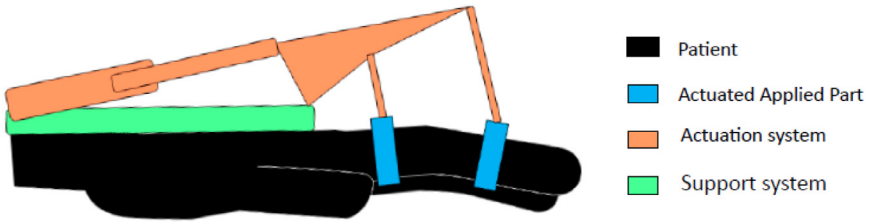

Fig. 8. Components of RobHand as a RACA robot (IEC).

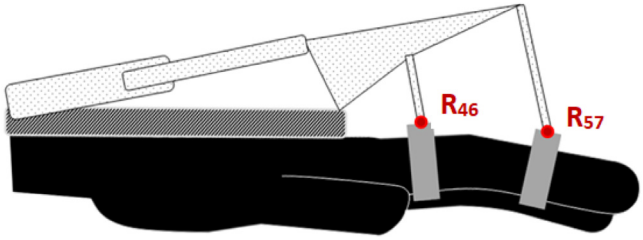

Fig. 9. RobHand Actuated Applied Parts (APPs) for one finger.

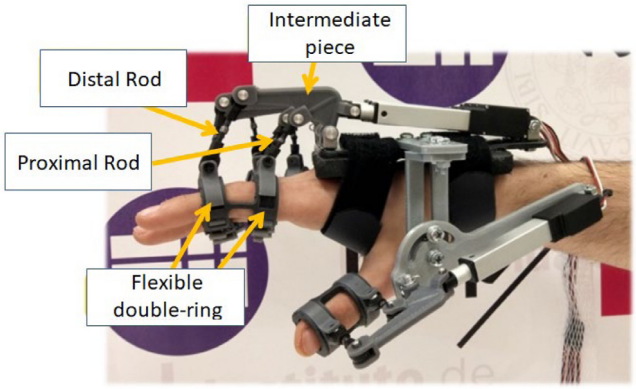

Fig. 10. Underactuated linkage-rotate mechanisms in the first prototype of the exoskeleton.

the kinematic model to maximize the ROM of each finger with compact size actuators and to achieve the highest performance in terms of the force transmission. The selected dimensions ensure that the center of rotation of each exoskeleton's subassembly is aligned with the center of rotation of each human's finger, or as close as possible. The use of underactuated mechanisms reduces the weight and cost of the exoskeleton due to the reduction in the number of actuators used.

RobHand is adjusted and immobilized on the patient's hand by using two Velcro straps jointed to the back support platform, and placed around the user hand palm and wrist. This allows the exoskeleton to be easily attached to the user hand, without any initial pose requirement of the fingers.

Many stroke patients suffer from hand spasticity. A usual consequence is that fingers remain closed, making a tight fist around the thumb, which is clenched into the palm. Thus, extending the hemiplegic patient's fingers to open their hands for putting on the exoskeleton is a difficult task. To ensure that the device can be easily placed in spastic hands, a flexible double-ring link (see Fig. 11) has been designed. Before starting a rehabilitation task, this flexible double-ring is placed on each of the patient's fingers, and then it is jointed to the corresponding linkage-rotate mechanism. It is composed by two rings and two connecting links. These connecting links ensure that the distance between both rings is constant, but they do not add new forces or torques on the finger.

The flexible double-ring allows PIP movements. It is characterized by three parameters: length (L) and diameters (D1, D2). L is the distance between the two rings, which is determined by the distance between the midpoints of the proximal and distal phalanges. D1 is designed according to the thickness of the proximal phalanx, and D2 according to the thickness of the medial phalanx. To ensure that the exoskeleton can be adapted to different finger sizes and geometries [61], three sets of double-rings (small, medium and large sizes for each finger) have been constructed. This allows the physical therapist an easy placement and adaptability, minimizing the time of exoskeleton placement at the beginning of a rehabilitation session.

The first prototype (showed in Fig. 10), was built from rapid prototyped parts, by means of additive manufacturing in 3D printing (Ultimaker® 2+). Its weight is 450 g in accordance with the indications set out in [52,62] (RobHand_VC2.mp4 is a short video clip showing in detail the RobHand exoskeleton). The linkage-rotate mechanism (intermediate piece and proximal and distal rods), the back support platform and the thumb module are built with Poly Lactic Acid (PLA). The double-rings, which are in direct contact with the human skin, are made of flexible material (Filaflex 82a), improving the ergonomics of the device. The prototype incorporates five Actuonix L12 linear actuators (DC motors with screw mechanism, 30 mm stroke, 23N output force, low-cost and lightweight). Referring to [63], and [64], the maximum force level of the human fingers was measured to be 50 N. Since the proposed hand exoskeleton is designed for the assistance of patients having a partially paralyzed hand, the required force level of the finger module is determined to be 10 N [64]. Thus, the selected linear actuators have sufficient capability to realize the required force.

During this development phase, usability and ergonomics tests were carried out with the collaboration of the Rehabilitation Service of the University Clinical Hospital (Valladolid, Spain). These tests were performed with five post-stroke patients (four man and one woman with ages between 30 and 60 years) who suffered from paresis in one of their hands (two in the left hand and three in the right one), and all in the chronic phase of the pathology. Four of them suffered from spasticity in the fingers with different levels of intensity. Sixty sessions of use of the exoskeleton were carried out with an approximate duration of sixty minutes each. Over the course of 20 weeks the patients underwent 3 weekly sessions. Fig. 12 shows the exoskeleton placed on the hands of two of the patients during the tests carried out.

During the indicated tests, due to the special characteristics of mobility and variety of the thumb size, the need to quickly position the mechanism responsible for the movement of this finger was detected. Therefore, the new mechanical design of the thumb module has two elements (see Fig. 13): a module on which the linear actuator and the intermediate piece are placed, and a mechanical device that joins this piece with the support platform. This mechanical element is a Noga LC6200 off-the-shelf device. It is a multi-articulated passive holder, that instantly

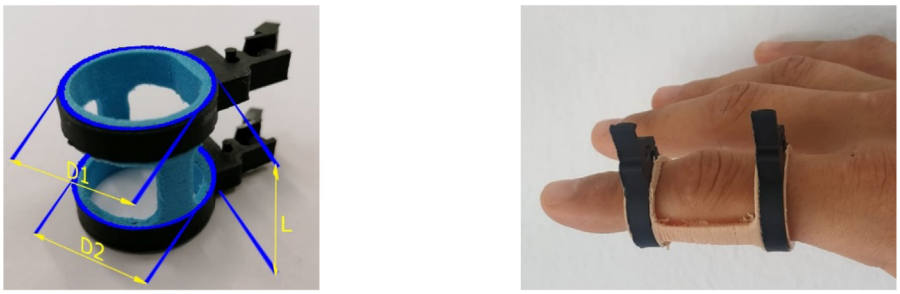

Fig. 11. Structure of flexible double-ring.

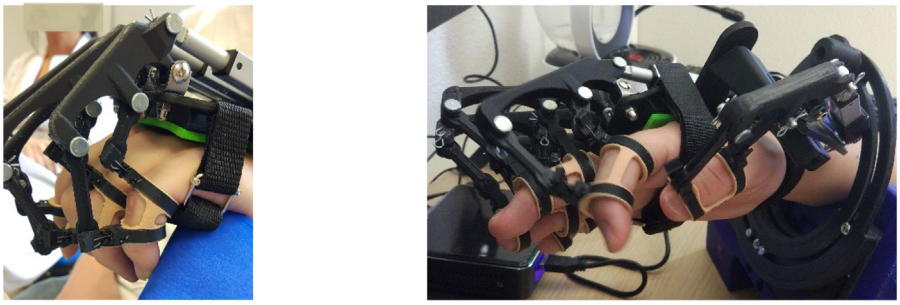

Fig. 12. Exoskeleton placed in the hands of two spastic patients during tests at the University Clinical Hospital (Valladolid, Spain).

Table 2
Weight of RobHand components (aluminum version).

Component	Quantity	Weight (g.)
Actuonix L12 Linear Actuator	5	170 (5 × 34)
Hand platform	1	236.6
Thumb subassembly platform	1	26.6
Intermediate piece	5	45 (5 × 9)
Proximal rod	5	3 (5 × 0.6)
Distal rod	5	9 (5 × 1.8)
Noga LC6200	1	85.62
Screws	1	34.3

fastens in any position, and has an easy set up into the required position. The position of this module with respect to the support platform is adjustable through a manual mechanism, providing an easy and quick adaptation to different thumb sizes. This allows an appropriate operation of the linear actuator that moves the thumb. This is an important advance, because many of the hand exoskeletons in the literature do not consider the thumb [39,65], or fail to provide a proper adaptation of the device to the thumb. (RobHand_VC3.mp4 is a short video clip showing the thumb placement and adjustment)

A second prototype (Fig. 13) was built in aluminum, using a 5-axis machining center. It weighs 610 g (weight of components is indicated in Table 2) and incorporates all the functional design advantages obtained in the development of the previous version.

6. Kinematic model validation

The developed kinematic model was verified performing tests using a single-finger 3D printed prototype (Ultimaker® 2+). The test consisted in calculating position and speed of selected points of interest by using Kinovea 0.8.26 that allows computing position, speed and acceleration of selected points from a video recording.

The validation of the kinematic model has been carried out comparing the results obtained by simulating the kinematic model (performed with Matlab®R2019a), and those obtained from tests performed with the prototype, using Kinovea.

Fig. 14 shows the set-up built to perform the test. Only the index finger has been considered because this finger offers a clean plane for measurements when the tests are recorded by a camera. The exoskeleton was coupled to a structure with its base in a horizontal position, and orthogonal to the recording plane. In this way the hand can remain still easily, making it easier to capture a quality video clip (RobHand_VC4.mp4 and RobHand_VC5.mp4 are two short video clips showing the processing with Kinovea to obtain experimental data).

Before starting the test with the prototype, the points of the exoskeleton whose parameters are to be analyzed throughout the test, are marked. To facilitate the identification of the points, a white glove has been placed over the hand. Two rotation points: R1 and R2 (this is the MCP joint), and four extra points: P1, P2, P3 and P4, have been chosen (see Fig. 14):

- P1: joint point between "intermediate piece" and "proximal rod"
- P2: joint point between "intermediate piece" and "linear actuator stroke"
- P3: joint point between "proximal ring" and "proximal rod"
- P4: joint point between "proximal ring" and "index finger".

The test involves the displacement of the linear actuator stroke from an initial position d = 16.5 mm, to a final position d = 39.7 mm. The complete test consists of a roundtrip path. The motion control of the linear actuator has been carried out with the Arduino® Mega 2565 controller.

Once the test is done, the recorded video is processed using Kinovea, to calculate the position and speed data of the selected points. The paths followed by points P1, P2, P4 and PIP are the circumferences shown in Fig. 14b. Angles and positions are calculated referred to the coordinate system located at the MCP joint (Fig. 14), since it can be considered a fixed point [50]. The analysis of this data, allows us to calculate:

- α angle of index finger. That is the MCP joint (angular position of proximal phalanx)

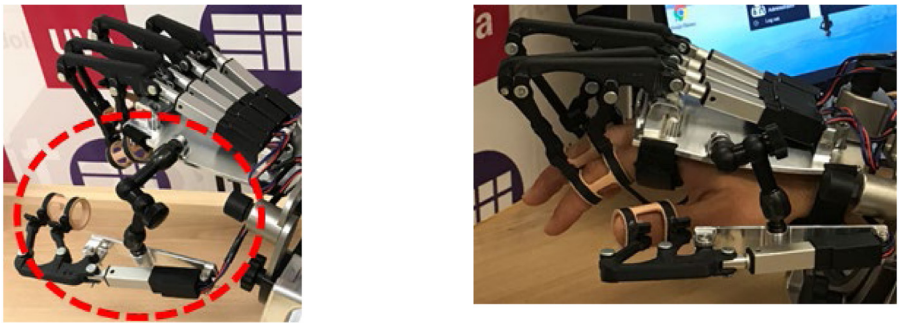

Fig. 13. Thumb module of second prototype of RobHand exoskeleton, manufactured in aluminum.

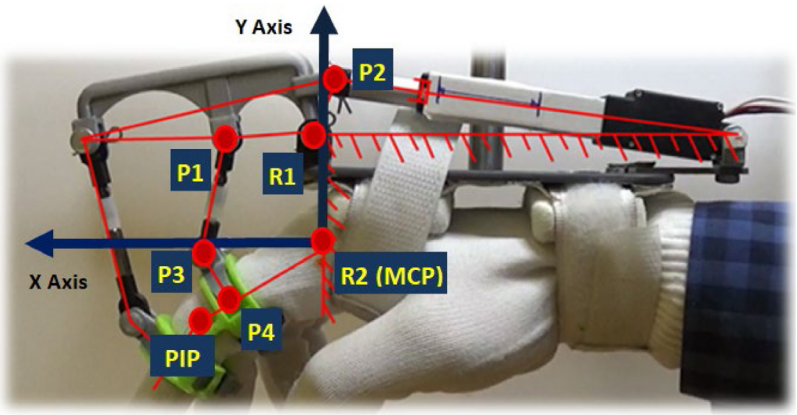

Fig. 14a. Set-up for performing tests with Kinovea.

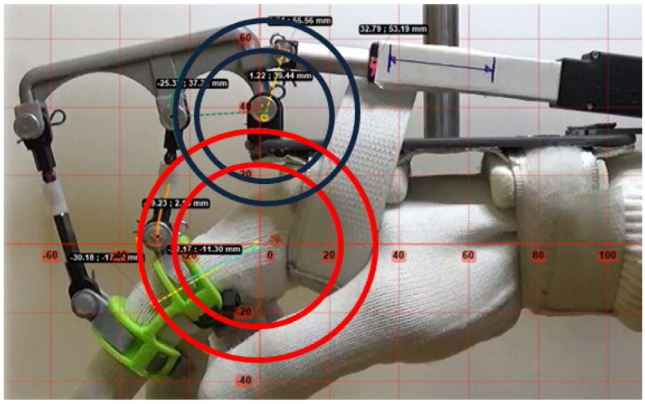

Fig. 14b. Circular paths described by selected points during the test.

- Index finger PIP joint coordinates: $(PIP_X, PIP_Y)_i$ i = 1, . . . n. That is, the horizontal position (PIP_X) and vertical position (PIP_Y) of PIP joint respect to the fixed reference system, located at the MCP joint.

The flow diagram to validate the kinematic model is showed in Fig. 15.

Fig. 16 shows a comparison of the values of the MCP joint (α_i) obtained by simulating the kinematic model of the exoskeleton with the data obtained by testing with the prototype. The brown line represents the values obtained by simulating the model with Matlab, and the blue one are the values obtained from Kinovea. These lines coincide in the central part of the figure, but there is a slight discrepancy between both angles in the initial and final parts. This is due to the small relative displacements that appear between the exoskeleton and the hand. It can also be observed in Fig. 16 that the RoM of the MCP joint is 8 ∼-62 degrees, which indicates the flexion of the finger reaches -62 degrees, and the extension reaches 8 degrees.

The error of MCP joint is defined as $MCP_{ERROR} = \alpha_{simulation} - \alpha_{prototype}$. Fig. 17 shows the evolution of this parameter as a function of the stroke extension (d). The maximum error is 3.5 degrees, which occurs at the beginning and at the end of the movement. Along the path, the error remains within the range [−2; 2] degrees. Fig. 18 indicates that the MCP joint relative error is less than 6.5%.

Fig. 19 shows the trajectory of the PIP joint on the XY plane. The brown line represents the simulated values and the blue one the experimental values. Both PIP paths are identical.

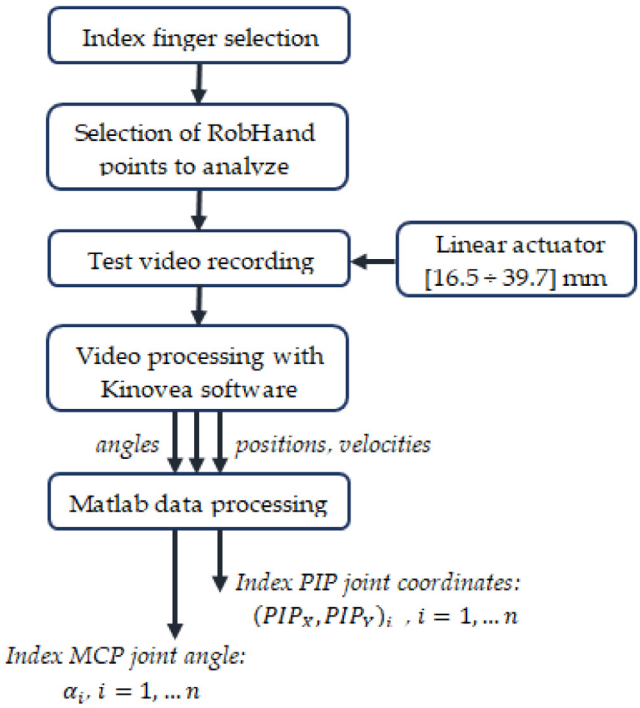

Fig. 15. Flow diagram of the kinematic model validation process.

7. Discussion

Results showed in Figs. 16–19 indicate that the obtained kinematic model is not entirely accurate but constitutes a good approximation to real behavior of the index finger of the prototype. The validation of kinematic model has only been presented for the index finger, but it is applicable to all fingers since the model is parameterizable. Indeed, to calculate RobHand's kinematic model, each finger has been modeled as the planar bar-linkage mechanism shown in Fig. 3.b. The linear and angular parameters that characterize the mechanism are indicated in Fig. 3.b and 3.c. Thus, just by modifying and adapting the value of these parameters to each finger, we can study their behavior. This gives great versatility to the developed kinematic model.

The validation of the kinematic model has been carried out by comparing the results obtained by simulation using Matlab, and those obtained with the tests performed with an index-finger prototype using Kinovea. The minor differences obtained and shown in Figs. 16–19 are due to several factors:

- The developed kinematic model relies on the assumption that the MCP joint is a fixed joint that does not move, which is not entirely true. This assumption is a good approximation because the shift that suffers the MCP joint during the flexion and extension of the finger is very slight and because of the difficulty of quantifying it.
- The model does not take into consideration deviations from the ideal configuration, such as the relative slippage of any part of the exoskeleton. The flexible rings may slide a little over the finger, which can lead variations in the values of some parameters. This is appreciated when observing the beginning and the end of Figs. 16 and 19, since theoretically the point should follow a circumference, and in practice this is not exactly the case. (see Fig. 14b).
- Monitoring of the selected points of the exoskeleton prototype is carried out using Kinovea, a specialized software package. These points "are not always the same" since the area used for monitoring has a square shape (side = 1 mm), and any point within that region is assumed to be correct. That is, some variation in the position of the zone to be monitored is allowed.

The dimensions of the planar-linkage mechanism have been calculated using the kinematic model, which has allowed reaching a balance between the achieved ROM and the size of the actuators (30 mm stroke). More precisely, the index finger can perform a maximum hyperextension movement of 8° and -5° at the MCP[α] and PIP [β] angles and a maximum flexion of −63° and -76° at the MCP[α] and PIP [β] joints, respectively. The obtained ROM is smaller than the natural ROM of the fingers (Table 1). However, it allows hyperextension (Figs. 16 and 19) and it is greater than the one reported in other related works. For example, the MCP angle of HoH varies from 0° to −55° with an actuator of 50 mm stroke, not allowing the hyperextension movement, which is essential for the treatment of people who experience flexor spasticity.

This result confirms the validity of our underactuated design to achieve both closing (flexion) and maximum opening (hyperextension) movements of the fingers. This feature is very useful for many stroke patients suffering from hand spasticity, since it allows rehabilitation tasks in which the exoskeleton helps to open and extend the fingers, thus facilitating the recovery of the spastic hand. In particular, the following actions can be performed:

- Hand opening and closing: flexion and extension of the five hand fingers simultaneously.
- Fingers opening and closing: flexion and extension of hand fingers individually
- Pinch grip and precision grip: flexion and extension of the thumb against index finger (precision grip) or against the four fingers (pinch grip).

Another advantage of our design in comparison with previous proposals is the possibility of performing well-conducted grips due to the integration of a multi-articulated passive holder (Noga LC6200 off-the-self device), that provides an easy adaptation of the thumb, which is a relevant aspect considering the great variability of the human hand dimensions.

8. Conclusions

This research proposes a novel exoskeleton for hand rehabilitation of hemiplegic stroke patients. It supports extension/flexion movements of the fingers by using an underactuated linkage-rotate mechanism that simplifies the design by using a single linear actuator per finger, resulting in lower device volume, weight and cost.

The mechanical design was a human-centered design process, focused on actual user requirements. Due to spasticity, the paretic hand of many hemiplegic patients is clasped into a fist at resting state. It is very difficult to extend the fingers of the patient to open the hand, and put on the exoskeleton. To solve this problem, a flexible double-ring link has been designed. To ensure the exoskeleton can be adapted to different finger sizes, three double-ring sets (small, medium and large sizes) have been constructed to adapt to the geometry of each patient's finger.

The thumb is the most complex finger of the hand and has special mobility characteristics of. Due to these reasons, it is difficult to ensure both, its comfortable integration in the exoskeleton, and that its movements are carried out adequately. We have developed a simple mechanism that easily adapts to the different sizes and length of the thumb, based on the Noga LC6200 off-the-self device, which provide an easy adaptation and integration of the thumb to the exoskeleton, achieving comfortable movements of the finger.

The obtained kinematic model allows to calculate the MCP [α] and PIP [β] joints values of each finger, as function of the known stroke extension of the linear actuator. It also allows us

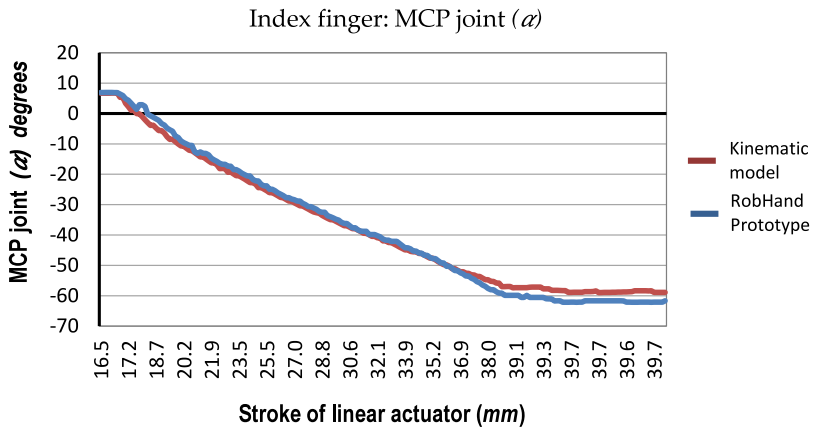

Fig. 16. MCP joint angle of index finger: comparative graph of results obtained by simulation of the kinematic model and by the prototype test.

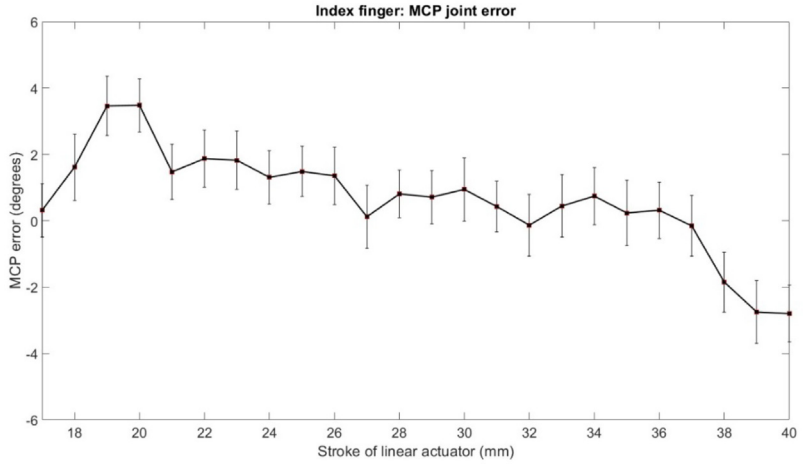

Fig. 17. Index finger: MCP joint error as a function of the stroke of the linear actuator (mean ± standard deviation).

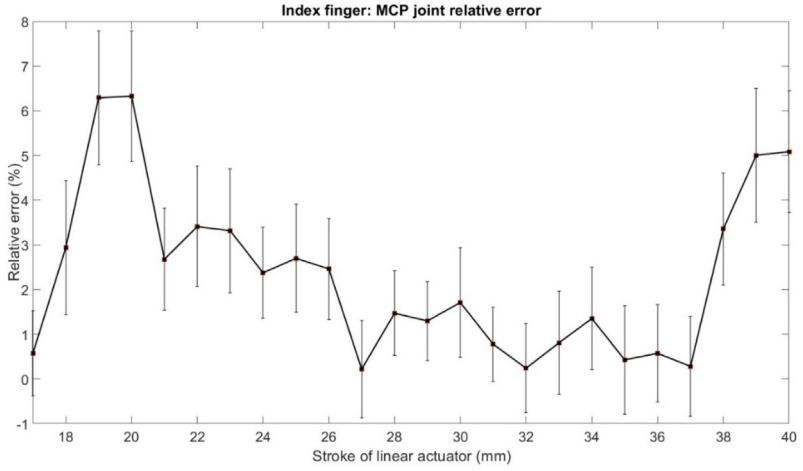

Fig. 18. Index finger: MCP joint relative error as a function of the stroke of the linear actuator.

to calculate the lengths of the rods (proximal and distal), for different sizes of the patient's fingers. This length is crucial, because if the rod length is shorter or longer than the one required by the patient, he may suffer discomfort and even new injuries derived from excessive turning. In addition, the application of the kinematic model has allowed us to achieve, with an underactuated design, ranges of motion that allow flexion and hyperextension and are suitable for the treatment of spastic patients.

Finally, the new concepts introduced by the IEC 80601-2-78 standard have been taken into account in its development, in particular the notion of "Actuated Applied Part" (AAP), essential when addressing efficiency and safety aspects in the design of

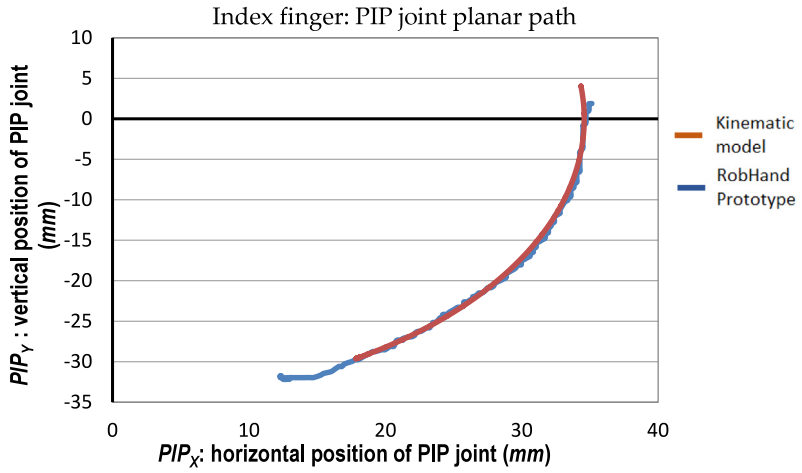

Fig. 19. Trajectory of the PIP joint of index finger on the XY plane: comparative graph of simulated and experimental results.

the exoskeleton. The AAPs have been identified in the mechanical structure and the model allows obtaining their geometric and kinematic parameters.

Funding

This work has been supported by CDTI, a Public Business Entity of the Spanish Ministry of Science and Innovation, by the European Regional Development Fund (ERDF) and by the company "CyL ImasD Informática S.L", under project IDI-20170263. It has also been partially funded by the Spanish Ministry of Science and Innovation through grant PID2019-111023RB-C33.

CRediT authorship contribution statement

Victor Moreno-SanJuan: Conceptualization, Mechanical design, Development of the kinematic model, Validation, Preparation and validation of the manuscript. **Ana Cisnal:** Conceptualization, Design implementation, Software, Preparation and validation of the manuscript. **Juan-Carlos Fraile:** Conceptualization, Methodology, Preparation and validation of the manuscript. **Javier Pérez-Turiel:** Conceptualization, Validation, Preparation and validation of the manuscript. **Eusebio de-la-Fuente:** Methodology, Preparation and validation of the manuscript.

Declaration of competing interest

The authors declare that they have no known competing financial interests or personal relationships that could have appeared to influence the work reported in this paper.

Acknowledgment

All authors approved the version of the manuscript to be published.

Appendix A. Supplementary data

Supplementary material related to this article can be found online at https://doi.org/10.1016/j.robot.2021.103828.

References

[1] World Health Organization, The top 10 causes of death, 2018, https://Www.Who.Int/News-Room/Fact-Sheets/Detail/the-Top-10-Causes-of-Death.
[2] W. Johnson, O. Onuma, M. Owolabi, S. Sachdev, Stroke: a global response is needed, Bull. World Health Organ. 94 (2016) https://doi.org/10.2471/BLT.16.181636.
[3] H. Nakayama, H. Stig Jørgensen, H. Otto Raaschou, T. Skyhøj Olsen, Recovery of upper extremity function in stroke patients: The Copenhagen stroke study, Arch. Phys. Med. Rehabil. 75 (1994) https://doi.org/10.1016/0003-9993(94)90161-9.
[4] T.B. Wyller, J. Holmen, P. Laake, K. Laake, Correlates of subjective well-being in stroke patients, Stroke 29 (1998) https://doi.org/10.1161/01.STR.29.2.363.
[5] E.J. Jonkman, A.W. Weerd, N.L.H. Vrijens, Quality of life after a first ischemic stroke, Acta Neurol. Scand. 98 (1998) https://doi.org/10.1111/j.1600-0404.1998.tb07289.x.
[6] D.T. Wade, R. Langton-Hewer, V.A. Wood, C.E. Skilbeck, H.M. Ismail, The hemiplegic arm after stroke: measurement and recovery., J. Neurol. Neurosurg. Psychiatry 46 (1983) https://doi.org/10.1136/jnnp.46.6.521.
[7] G. Kwakkel, B.J. Kollen, R.C. Wagenaar, Long term effects of intensity of upper and lower limb training after stroke: a randomised trial, J. Neurol. Neurosurg. Psychiatry 72 (2002) 473–479.
[8] C.A. Trombly, Occupational Therapy for Physical Dysfunction, sixth ed., Williams & Wilkins, London, 2003.
[9] N. Takeuchi, S.-I. Izumi, Rehabilitation with poststroke motor recovery: A review with a focus on neural plasticity, Stroke Res. Treat. 2013 (2013) https://doi.org/10.1155/2013/128641.
[10] H. Kawasaki, S. Ueki, S. Ito, T. Mouri, Design and Control of a Hand-Assist Robot with Multiple Degrees of Freedom for Rehabilitation Therapy, in: Robot. Syst., IGI Global, 2020, https://doi.org/10.4018/978-1-7998-1754-3.ch043.
[11] J.M. Veerbeek, A.C. Langbroek-Amersfoort, E.E.H. van Wegen, C.G.M. Meskers, G. Kwakkel, Effects of robot-assisted therapy for the upper limb after stroke, Neurorehabil. Neural Repair. 31 (2017) https://doi.org/10.1177/1545968316666957.
[12] F. Aggogeri, T. Mikolajczyk, J. O'Kane, Robotics for rehabilitation of hand movement in stroke survivors, Adv. Mech. Eng. 11 (2019) https://doi.org/10.1177/1687814019841921.
[13] ISO TC 299 WG5 (jointly with IEC/TC6), IEC 80601-2-78:2019. Medical electrical equipment — Part 2-78: Particular requirements for basic safety and essential performance of medical robots for rehabilitation, assessment, compensation or alleviation, first ed., 2019.
[14] D.G. Kamper, R.L. Harvey, S. Suresh, W.Z. Rymer, Relative contributions of neural mechanisms versus muscle mechanics in promoting finger extension deficits following stroke, Muscle Nerve 28 (2003) https://doi.org/10.1002/mus.10443.
[15] J.G. Colebatch, S.C. Gandevia, The distribution of muscular weakness in upper motor lesions affecting the arm, Brain 112 (1989) https://doi.org/10.1093/brain/112.3.749.
[16] L. Ada, C.G. Canning, S.-L. Low, Stroke patients have selective muscle weakness in shortened range, Brain 126 (2003) https://doi.org/10.1093/brain/awg066.

[17] M.A. Gull, S. Bai, T. Bak, A review on design of upper limb exoskeletons, Robotics 9 (2020) 1–35, https://doi.org/10.3390/robotics9010016.

[18] F. Aggogeri, T. Mikolajczyk, J. O'Kane, Robotics for rehabilitation of hand movement in stroke survivors, Adv. Mech. Eng. 11 (2019) 168781401984192, https://doi.org/10.1177/1687814019841921.

[19] R.J. Varghese, D. Freer, F. Deligianni, J. Liu, G.-Z. Yang, Wearable robotics for upper-limb rehabilitation and assistance: A review of the state-of-the-art, challenges and future research, in: Wearable Technol. Med. Health Care, Elsevier, 2018, p. 340, https://www.elsevier.com/books/wearable-technology-in-medicine-and-health-care/tong/978-0-12-811810-8.

[20] T. Proietti, V. Crocher, A. Roby-Brami, N. Jarrasse, Upper-limb robotic exoskeletons for neurorehabilitation: A review on control strategies, IEEE Rev. Biomed. Eng. 9 (2016) 4–14, https://doi.org/10.1109/RBME.2016.2552201.

[21] P.W. Ferguson, Y. Shen, J. Rosen, Hand exoskeleton systems—Overview, in: Y. Shen (Ed.), Wearable Robot, Academic Press, 2020, pp. 149–175, https://doi.org/10.1016/B978-0-12-814659-0.00008-4.

[22] B. Noronha, D. Accoto, Exoskeletal devices for hand assistance and rehabilitation: a comprehensive analysis of state-of-the-art technologies, IEEE Trans. Med. Robot. Bionics (2021) 1, https://doi.org/10.1109/tmrb.2021.3064412.

[23] T. du Plessis, K. Djouani, C. Oosthuizen, A review of active hand exoskeletons for rehabilitation and assistance, Robotics 10 (2021) 40, https://doi.org/10.3390/robotics10010040.

[24] C. da Cruz Teixeira, J. Cavalcante de Oliveira, Right hand rehabilitation with CyberForce, CyberGrasp, and CyberGlove, in: 2015 XVII Symp. Virtual Augment. Real, IEEE, 2015, https://doi.org/10.1109/SVR.2015.34.

[25] N.S.K. Ho, K.Y. Tong, X.L. Hu, K.L. Fung, X.J. Wei, W. Rong, E.A. Susanto, An EMG-driven exoskeleton hand robotic training device on chronic stroke subjects: Task training system for stroke rehabilitation, in: 2011 IEEE Int. Conf. Rehabil. Robot, IEEE, Zurich, Switzerland, 2011, pp. 1–5, https://doi.org/10.1109/ICORR.2011.5975340.

[26] A. Borboni, M. Mor, R. Faglia, Gloreha—Hand robotic rehabilitation: Design, mechanical model, and experiments, J. Dyn. Syst. Meas. Control 138 (2016) https://doi.org/10.1115/1.4033831.

[27] D. Wang, Q. Meng, Q. Meng, X. Li, H. Yu, Design and development of a portable exoskeleton for hand rehabilitation, IEEE Trans. Neural Syst. Rehabil. Eng. 26 (2018) https://doi.org/10.1109/TNSRE.2018.2878778.

[28] L. Cheng, M. Chen, Z. Li, Design and control of a wearable hand rehabilitation robot, IEEE Access 6 (2018) https://doi.org/10.1109/ACCESS.2018.2884451.

[29] Y.-K. Ou, Y.-L. Wang, H.-C. Chang, C.-C. Chen, Design and development of a wearable exoskeleton system for stroke rehabilitation, Healthcare 8 (2020) https://doi.org/10.3390/healthcare8010018.

[30] G. Carbone, E.C. Gerding, B. Corves, D. Cafolla, M. Russo, M. Ceccarelli, Design of a two-DOFs driving mechanism for a motion-assisted finger exoskeleton, Appl. Sci. 10 (2020) https://doi.org/10.3390/app10072619.

[31] C. Morales-Cruz, C.E. Capalbo, G. Caroleo, M. Ceccarelli, G. Carbone, Numerical and Experimental Validation of ExoFing, a Finger Exoskeleton, 2020, https://doi.org/10.1007/978-3-030-55061-5_14.

[32] C.N. Schabowsky, S.B. Godfrey, R.J. Holley, P.S. Lum, Development and pilot testing of HEXORR: Hand exoskeleton rehabilitation robot, J. Neuroeng. Rehabil. 7 (2010) https://doi.org/10.1186/1743-0003-7-36.

[33] A. Chiri, F. Giovacchini, N. Vitiello, E. Cattin, S. Roccella, F. Vecchi, M.C. Carrozza, HANDEXOS: Towards an exoskeleton device for the rehabilitation of the hand, in: 2009 IEEE/RSJ Int. Conf. Intell. Robot. Syst, IEEE, 2009, https://doi.org/10.1109/IROS.2009.5354376.

[34] C.D. Takahashi, L. Der-Yeghiaian, V.H. Le, S.C. Cramer, A Robotic Device for Hand Motor Therapy after Stroke, in: 9th Int. Conf. Rehabil. Robot. 2005. ICORR 2005., in: IEEE, n.d. https://doi.org/10.1109/ICORR.2005.1501041.

[35] T. Laliberté, L. Birglen, C. Gosselin, Underactuation in robotic grasping hands, Mach. Intell. Robot. Control 4 (2002) 1–11, https://www.researchgate.net/profile/Clement_Gosselin/publication/234047273_Underactuation_in_robotic_grasping_hands'/links/5420107e0cf2218008d43916.pdf (Accessed 22 February 2019).

[36] P.J. Kyberd, A. Clawson, B. Jones, The use of underactuation in prosthetic grasping, Mech. Sci. 2 (2011) https://doi.org/10.5194/ms-2-27-2011.

[37] L. Birglen, T. Laliberté, C. Gosselin, Underactuated Robotic Hands, Springer Berlin Heidelberg, Berlin, Heidelberg, 2008, https://doi.org/10.1007/978-3-540-77459-4.

[38] M.B. Hong, S.J. Kim, Y.S. Ihn, G.-C. Jeong, K. Kim, KULEX-Hand: An underactuated wearable hand for grasping power assistance, IEEE Trans. Robot. 35 (2019) https://doi.org/10.1109/TRO.2018.2880121.

[39] M. Sarac, M. Solazzi, E. Sotgiu, M. Bergamasco, A. Frisoli, Design and kinematic optimization of a novel underactuated robotic hand exoskeleton, Meccanica 52 (2017) 749–761, https://doi.org/10.1007/s11012-016-0530-z.

[40] M. Gabardi, M. Solazzi, D. Leonardis, A. Frisoli, Design and evaluation of a novel 5 DoF underactuated thumb-exoskeleton, IEEE Robot. Autom. Lett. 3 (2018) 2322–2329, https://doi.org/10.1109/LRA.2018.2807580.

[41] Y. Jin, Y. Zhao, Post-stroke upper limb spasticity incidence for different cerebral infarction site, Open Med. 13 (2018) https://doi.org/10.1515/med-2018-0035.

[42] J. Wissel, A. Manack, M. Brainin, Toward an epidemiology of post-stroke spasticity, Neurology 80 (2013) https://doi.org/10.1212/WNL.0b013e3182762448.

[43] X.Q. Shi, H.L. Heung, Z.Q. Tang, Z. Li, K.Y. Tong, Effects of a soft robotic hand for hand rehabilitation in chronic stroke survivors, J. Stroke Cerebrovasc. Dis. 30 (2021) https://doi.org/10.1016/j.jstrokecerebrovasdis.2021.105812.

[44] M.S. Erden, W. McColl, D. Abassebay, S. Haldane, Hand exoskeleton to assess hand spasticity, in: 2020 8th IEEE RAS/EMBS Int. Conf. Biomed. Robot. Biomechatronics, IEEE, 2020, https://doi.org/10.1109/BioRob49111.2020.9224329.

[45] S. Kim, J. Lee, J. Bae, Analysis of finger muscular forces using a wearable hand exoskeleton system, J. Bionic Eng. 14 (2017) https://doi.org/10.1016/S1672-6529(16)60434-1.

[46] R. de-la Torre, E.D. Oña, C. Balaguer, A. Jardón, Robot-aided systems for improving the assessment of upper limb spasticity: A systematic review, Sensors 20 (2020) https://doi.org/10.3390/s20185251.

[47] Y.-L. Tsai, J.-J. Huang, S.-W. Pu, H.-P. Chen, S.-C. Hsu, J.-Y. Chang, Y.-C. Pei, Usability assessment of a cable-driven exoskeletal robot for hand rehabilitation, Front. Neurorobot. 13 (2019) https://doi.org/10.3389/fnbot.2019.00003.

[48] K. Monaghan, F. Horgan, C. Blake, C. Cornall, P.P. Hickey, B.E. Lyons, P. Langhorne, Physical treatment interventions for managing spasticity after stroke, Cochrane Database Syst. Rev. (2017) https://doi.org/10.1002/14651858.CD009188.pub2.

[49] K.Y. Tong, S.K. Ho, P.M.K. Pang, X.L. Hu, W.K. Tam, K.L. Fung, X.J. Wei, P.N. Chen, M. Chen, An intention driven hand functions task training robotic system, in: 2010 Annu. Int. Conf. IEEE Eng. Med. Biol, IEEE, 2010, https://doi.org/10.1109/IEMBS.2010.5627930.

[50] J.J. LaViola, A Survey of Hand Posture and Gesture Recognition Techniques and Technology, Providence, RI, United States, 1999.

[51] K. Andrianesis, A. Tzes, Development and control of a multifunctional prosthetic hand with shape memory alloy actuators, J. Intell. Robot. Syst. 78 (2015) https://doi.org/10.1007/s10846-014-0061-6.

[52] P.M. Aubin, H. Sallum, C. Walsh, L. Stirling, A. Correia, A pediatric robotic thumb exoskeleton for at-home rehabilitation: The isolated orthosis for thumb actuation (IOTA), in: 2013 IEEE 13th Int. Conf. Rehabil. Robot, IEEE, 2013, https://doi.org/10.1109/ICORR.2013.6650500.

[53] J.M. Ochoa, Yicheng Jia, D. Narasimhan, D.G. Kamper, Development of a portable actuated orthotic glove to facilitate gross extension of the digits for therapeutic training after stroke, in: 2009 Annu. Int. Conf. IEEE Eng. Med. Biol. Soc, IEEE, 2009, https://doi.org/10.1109/IEMBS.2009.5333630.

[54] M. Sarac, M. Solazzi, A. Frisoli, Design requirements of generic hand exoskeletons and survey of hand exoskeletons for rehabilitation, assistive, or haptic use, IEEE Trans. Haptics. 12 (2019) https://doi.org/10.1109/TOH.2019.2924881.

[55] P. Heo, G.M. Gu, S. Lee, K. Rhee, J. Kim, Current hand exoskeleton technologies for rehabilitation and assistive engineering, Int. J. Precis. Eng. Manuf. 13 (2012) https://doi.org/10.1007/s12541-012-0107-2.

[56] S. Cobos, M. Ferre, M.A. Sanchez Uran, J. Ortego, C. Pena, Efficient human hand kinematics for manipulation tasks, in: 2008 IEEE/RSJ Int. Conf. Intell. Robot. Syst, IEEE, 2008, https://doi.org/10.1109/IROS.2008.4651053.

[57] N.J. Jarque-Bou, M. Atzori, H. Müller, A large calibrated database of hand movements and grasps kinematics, Sci. Data 7 (2020) https://doi.org/10.1038/s41597-019-0349-2.

[58] M.O. Ajayi, K. Djouani, Y. Hamam, Interaction control for human-exoskeletons, J. Control Sci. Eng. 2020 (2020) https://doi.org/10.1155/2020/8472510.

[59] N. Jarrasse, G. Morel, Connecting a human limb to an exoskeleton, IEEE Trans. Robot. 28 (2012) https://doi.org/10.1109/TRO.2011.2178151.

[60] J. Bird, C. Ross, Mechanical Engineering Principles, second ed., Taylor and Francis, Hoboken, NJ, 2012.

[61] O. Sandoval-Gonzalez, J. Jacinto-Villegas, I. Herrera-Aguilar, O. Portillo-Rodiguez, P. Tripicchio, M. Hernandez-Ramos, A. Flores-Cuautle, C. Avizzano, Design and development of a hand exoskeleton robot for active and passive rehabilitation, Int. J. Adv. Robot. Syst. 13 (2016) https://doi.org/10.5772/62404.

[62] C.J. Nycz, T. Butzer, O. Lambercy, J. Arata, G.S. Fischer, R. Gassert, Design and characterization of a lightweight and fully portable remote actuation system for use with a hand exoskeleton, IEEE Robot. Autom. Lett. 1 (2016) https://doi.org/10.1109/LRA.2016.2528296.

[63] J. Iqbal, N.G. Tsagarakis, D.G. Caldwell, A human hand compatible optimised exoskeleton system, in: 2010 IEEE Int. Conf. Robot. Biomimetics, IEEE, 2010, https://doi.org/10.1109/ROBIO.2010.5723409.
[64] S. Ueki, H. Kawasaki, S. Ito, Y. Nishimoto, M. Abe, T. Aoki, Y. Ishigure, T. Ojika, T. Mouri, Development of a hand-assist robot with multi-degrees-of-freedom for rehabilitation therapy, IEEE/ASME Trans. Mechatronics 17 (2012) https://doi.org/10.1109/TMECH.2010.2090353.
[65] A. Lince, N. Celadon, A. Battezzato, A. Favetto, S. Appendino, P. Ariano, M. Paleari, Design and testing of an under-actuated surface EMG-driven hand exoskeleton, in: 2017 Int. Conf. Rehabil. Robot. IEEE, 2017, https://doi.org/10.1109/ICORR.2017.8009325.

Victor Moreno-SanJuan completed the B.S. degree in Mechanical Engineering in 2018 and the M.S. studies in Industrial Engineering in 2020 at the University of Valladolid (Valladolid, Spain). He is currently doing his Ph.D. studies at the School of Industrial Engineering of the University of Valladolid. He has done research work at the Instituto de las Tecnologías Avanzadas de la Producción since 2018 where he worked until 2020. He is currently researching the developments of robotic platforms for laparoscopic surgery.

Ana Cisnal received the B.S. degree in Industrial Electronics and Automation Engineering in 2017 and the M.S. degree in Industrial Engineering in 2019, both from the University of Valladolid (Spain). She is currently pursuing the Ph.D. degree at the University of Valladolid. During 2016, she participated in qualities internships at Fraunhofer IBMT (Sankt Ingbert, Germany). From 2017 until now, she has been working at the ITAP Institute of the University of Valladolid as a research fellowship and contract researcher. She became IEEE Student Member in 2018. Her research line focuses in the bio-cooperative control of robotic neuromotor rehabilitation platforms.

J.C. Fraile received the Ph.D. Degree in Control Engineering from the Faculty of Engineering, University of Valladolid, Spain, in 1987. Since 1992, he has been an Associate Professor of control and robotics in the Faculty of Engineering, University of Valladolid. In 1998 he was holding a visiting professor position at ICES. Institute for Complex Engineering Systems, Carnegie Mellon University, Pittsburgh, USA. Hi is leader of the ITAP-Medical Robotics group at University of Valladolid. His current research interests include rehabilitation robotics and robots for surgery.

Javier Pérez Turiel is Associate Professor at the Department of Systems Engineering of the University of Valladolid (Spain) ehere he received the Ph.D. Degree in Control Engineering in 1994. In 1999 he was visiting professor at the Electrical Engineering and Computer Science Dpt. (EECS), University of Michigan (US). He has been the Head of the Biomedical Engineering Division at CARTIF Technological Centre from 2000 to 2014. He is also member of the Medical Robotics group at ITAP (Institute of Advanced Production Technologies) University Institute. His research interests include surgical and rehabilitation robotics.

Eusebio de la Fuente received his M.Sc. in 1991 in electronic engineering and automatic control and Ph.D. in 1997, both from University of Valladolid (Spain). Since 1999 he is an Associate Professor in computer science with specialization in computer vision at Industrial Engineering School in Valladolid (Spain). His current research interests lie in the field of medical image processing and real-time video analysis for rehabilitation and surgical robot applications. He is specially interested in deep learning techniques for object detection in medical images and classification.